GA–A26472

MEASUREMENT AND MODELING OF TEARING MODE STABILITY FOR STEADY-STATE PLASMAS IN DIII-D

by
F. TURCO, T.C. LUCE, J.R. FERRON, C.C. PETTY, P.A. POLITZER, A.D. TURNBULL,
D.P. BRENNAN, M. MURAKAMI, L. LODESTRO, D. PEARLSTEIN, T.A. CASPER,
R.J. JAYAKUMAR, and C.T. HOLCOMB

JULY 2009

GENERAL ATOMICS

DISCLAIMER

GA–A26472

MEASUREMENT AND MODELING OF TEARING MODE STABILITY FOR STEADY-STATE PLASMAS IN DIII-D

by

F. TURCO,* T.C. LUCE, J.R. FERRON, C.C. PETTY, P.A. POLITZER, A.D. TURNBULL,
D.P. BRENNAN,† M. MURAKAMI,‡ L. LODESTRO,¶ D. PEARLSTEIN,¶ T.A. CASPER,¶
R.J. JAYAKUMAR,¶ and C.T. HOLCOMB¶

This is a preprint of a paper presented at the 36th EPS Conf. on Plasma Physics, in Sofia, Bulgaria, June 29th through July 3, 2009 and to be published in the *Proceedings.*

*Oak Ridge Institute for Science Education, Oak Ridge, Tennessee.
†University of Tulsa, Tulsa, Oklahoma.
‡Oak Ridge National Laboratory, Oak Ridge, Tennessee.
¶Lawrence Livermore National Laboratory, Livermore, California.

Work supported by
the U.S. Department of Energy
under DE-AC05-06OR23100, DE-FC02-04ER54698,
DE-AC05-00OR22725, and DE-AC52-07NA27344

GENERAL ATOMICS PROJECT 30200
JULY 2009

GENERAL ATOMICS

Measurement and Modelling of Tearing Mode Stability for Steady-State Plasmas in DIII-D

F. Turco[1], T.C. Luce[2], J.R. Ferron[2], C.C. Petty[2], P.A. Politzer[2], A.D. Turnbull[2],
D.P. Brennan[3], M. Murakami[4], L.L. Lodestro[5], L.D. Pearlstein[5], T.A. Casper[5],
R.J. Jayakumar[5], and C.T. Holcomb[5]

[1]*Oak Ridge Associated Universities, Oak Ridge, Tennessee, USA*
[2]*General Atomics, PO Box 85608, San Diego, California 92186-5608, USA*
[3]*University of Tulsa, Tulsa, Oklahoma, USA*
[4]*Oak Ridge National Laboratory, Oak Ridge, Tennessee, USA*
[5]*Lawrence Livermore National Laboratory, Livermore, California 94551, USA*

Introduction

High-beta, quasi-steady state scenarios represent a fundamental step towards the performance required for future fusion reactors. In DIII-D steady-state scenario discharges, the normalised beta $\beta_N \equiv \beta(\%) \cdot a(m) \cdot B_T(T)/I_p(\mathrm{MA})$ (where β is the ratio of the plasma pressure to the magnetic field pressure, a the plasma minor radius, B_T the toroidal magnetic field and I_p the plasma current) exceeds the no-wall ideal kink beta limit. The performance of this scenario is limited by the onset of an n=1 tearing mode, which appears on the resistive evolution time-scale (1–2 s) at constant pressure and causes both a loss of confinement and a radial redistribution of the current density from which the available current drive sources cannot recover. It is routinely observed that the injection of electron cyclotron current drive (ECCD) with a broad deposition can prevent the mode from appearing. This is not a case of a direct stabilisation due to the interaction with the mode's rational surface. These variations of the scenario are illustrated in Fig. 1, where the total injected power [neutral beam injection (NBI) and ECCD], β_N and the n=1 magnetic perturbation at the outer wall are shown. In case (a), the onset of the n=1 mode is observed when the EC power is not present or if it is stopped before the end of the high β phase, whereas in case (b) the difference is pointed out between

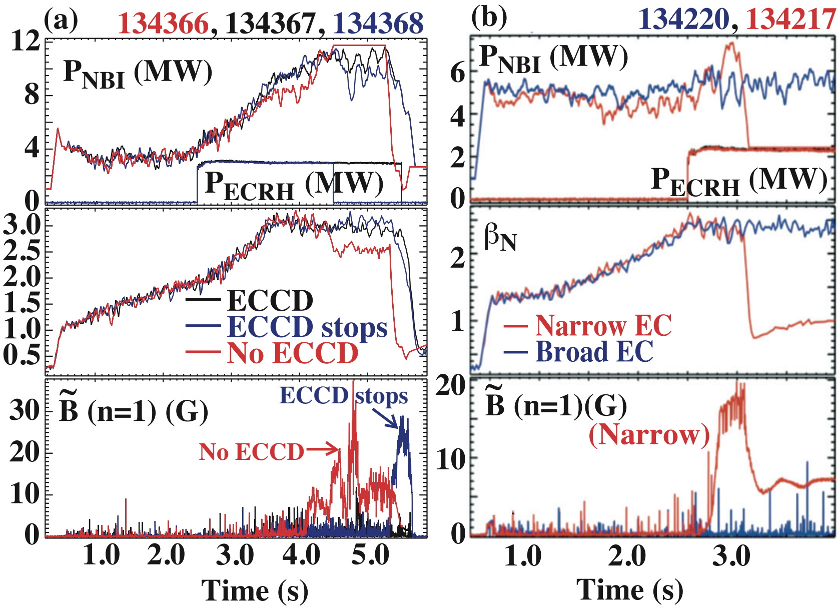

Fig. 1. Evolution of NBI and EC power (first row), β_N (second row), n=1 MHD activity by Mirnov coils signals (third row) for cases with different ECCD (a) timing (b) deposition width.

broad and narrow current deposition (the case narrow deposition becoming unstable). The current density profile evolution and the MHD modes of several sets of significant discharges with and without ECCD (at different locations) have been analysed, using motional Stark effect (MSE) spectroscopy measurements for the former and edge magnetic probes measurements, toroidal rotation profiles and fast electron cyclotron emission (ECE) data for the latter. One equilibrium based on EFIT reconstruction [1] with kinetic data has been perturbed by adding local current density at a specific radius, mimicking the application of EC waves, and the changes in the stability for a sequence of equilibria with the current perturbed at various radii, have been evaluated by the DCON [2], GATO [3] and PEST3 [4] codes.

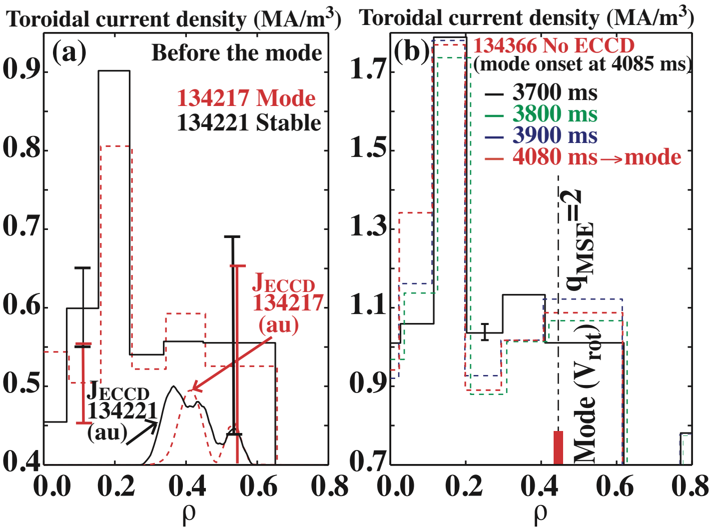

Fig. 2. MSE reconstructed current profiles for discharges (a) #134217 (red, unstable), #134221 (black, stable) and (b) #134366 (evolution until the mode onset in red). A systematic error seems to affect the channels at ρ≳0.7 so they are not shown. Error bars are indicated by vertical lines.

The Role of ∇*j*

A pattern has been found, common to most of the discharges regardless of the characteristics of the background current profile, that relates the change of the local gradient of the toroidal current density, ∇*j*, to the discharge instability. An increasing current density gradient, of either sign and localised just inside the mode position (usually at the q=2 surface in the analysed database), characterises the unstable discharges. In particular, a narrow EC current deposition is expected to create a local current build-up, while a broad deposition would keep the profile smoother. In Fig. 2(a) the toroidal current density points from MSE measurements are shown, for a discharge with narrow EC deposition (red traces), just before a 2/1 mode develops, and a stable one, with broad EC deposition (black traces). The same holds in the case of an increasingly negative ∇*j* that, as in the case shown in Fig. 2(b), might be the result of a n=2 mode detected at ρ~0.4. In the absence of EC current, a localised reversal of the gradient develops, which drives a 2/1 mode of high amplitude unstable. The subsequent discharge, repeated with broad EC current deposition, remains stable, because the EC current prevents the *j* profile from becoming locally inverted. The current profile evolution, in some cases affected by significant error bars, is always checked against the MSE pitch angle time histories, which confirm the conclusion about the impact of ∇*j* on the stability of the discharges. A statistical study has been carried out on a series of repeated discharges (among which two show the appearance of a mode at $\rho\sim0.55$), which evaluates the difference between the local ∇j of the unstable and the stable discharges. The discharges in Fig. 2(a) are taken within that dataset, while #134366 in Fig. 2(b) is not part of this study. A structure appears just inside the mode position, indicating that a higher current gradient at that location is a recurrent feature within the unstable discharges (Fig. 3). Conversely, the pressure profiles of the analysed cases remain constant up to the time of the mode onset, and do not differ from the profiles of the stable discharges. Thus, although the discharges are above the free boundary limit, instabilities appear to be mainly driven by large ∇j, of either sign, past inside the rational surface.

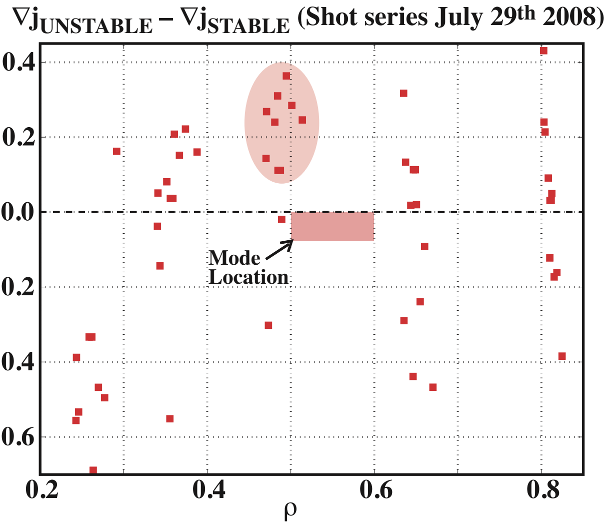

Fig. 3. Differences between local current gradients of unstable discharges at the time of the mode onset, and of stable discharges at the same time slice. The shaded area highlights the series of $\nabla j_{\mathrm{unstable}} > \nabla j_{\mathrm{stable}}$.

Resistive MHD Analysis

The radial structure of the modes indicates that most of the instabilities are m/n=2/1 or 3/1 tearing modes. The kinetic reconstruction of one equilibrium was perturbed by a series of localised Gaussian perturbations of the current, positioned from $\rho\sim0.06$–0.965 and with amplitudes varying from 4% to 16% of the total current. The ideal stability calculations (performed with DCON and GATO) indicate that the unperturbed equilibrium is ideally unstable to an n=1 mode without a wall, and slightly below the ideal-wall stability limit. For this reason, the tearing stability index Δ' might be very sensitive to the equilibrium characteristics [5]. The stability calculations were performed with a conformal wall positioned at a distance from the plasma that was found previously to best match the behaviour of the DIII-D vessel wall. We focussed our study on the q=2 surface alone, as velocity shear is likely to screen coupling to the other surfaces. One matching matrix containing the interchange and resistive terms has been calculated for every radial deposition of EC current (~100 radial points). The results for Δ' around the q=2 position and the ∇j obtained when the perturbation is located at the q=2 surface are plotted in Fig. 4, for one perturbation scan of small amplitude ($I_{\mathrm{EC}}/I_{\mathrm{tot}} = f_{\mathrm{EC}} \sim 6\%$) — which produces gradients comparable to the experimental ∇j observed in the MSE data — and for a broad EC deposition injected at $\rho\sim0.25$–0.55. The resistive index grows to its maximum at the points where the current gradient at the position of q=2 deviates most from the unperturbed profile. This is consistent with the observation of higher instability in the discharges when a higher ∇j, of either sign, is observed. Conversely, perturbations at the rational surface show a significant stabilisation ($\Delta' \ll 0$), although $\nabla j_{q=2} \approx \nabla j_{unperturbed}$ in those cases. The broad EC current deposition does not modify the ∇*j* at *q*=2 significantly, but the corresponding Δ′ is higher than the unperturbed level. This indicates that the current gradient at *q*=2 is not the only drive for instability. It appears that any ∇*j* perturbation lying more than ~5% of the minor radius away from the rational surface does not affect the stability of the mode. This is consistent with the results obtained previously in a similar study with an analytical model for cylindrical geometry by Westerhof [6], compared to the PEST3 results in Fig. 5 (the points are extracted from Fig. 2 in Ref. 5). The toroidal geometry seems to impact only the amplitude of the calculated Δ´ and so far the resistive stability is affected only by local parameters. We are also evaluating the way PEST3 deals with the effects of the ideal stability of the equilibrium, which might ultimately affect the results for the resistive stability. Inner-layer calculations to determine whether this level of Δ´ is sufficient for a growing tearing mode are also in progress.

This work was supported in part by the US Department of Energy under DE-AC05-06OR23100, DE-FC02-04ER54698, DE-AC05-00OR22725, and DE-AC52-07NA27344.

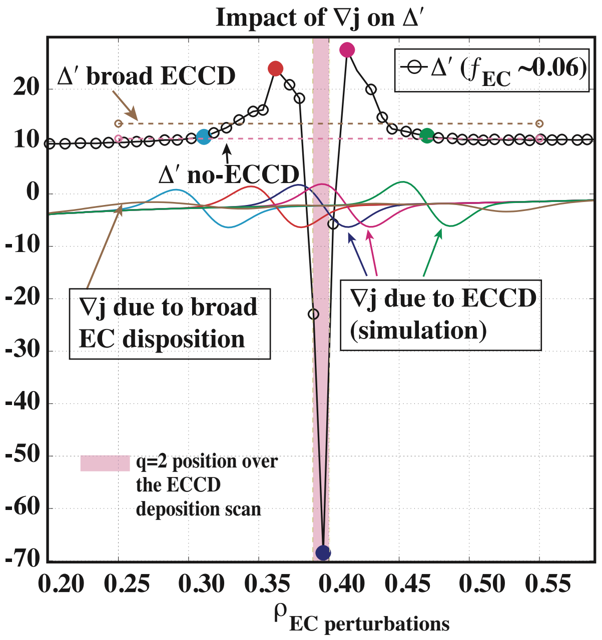

FIG. 4. Δ´ values for all simulated ECCD depositions (black f_{EC}~0.06, brown broad f_{EC}, pink no ECCD) and ∇*j* for ECCD dispositions around the *q*=2 rational surface. The coloured circles correspond to the matching colour for the ∇*j* trace.

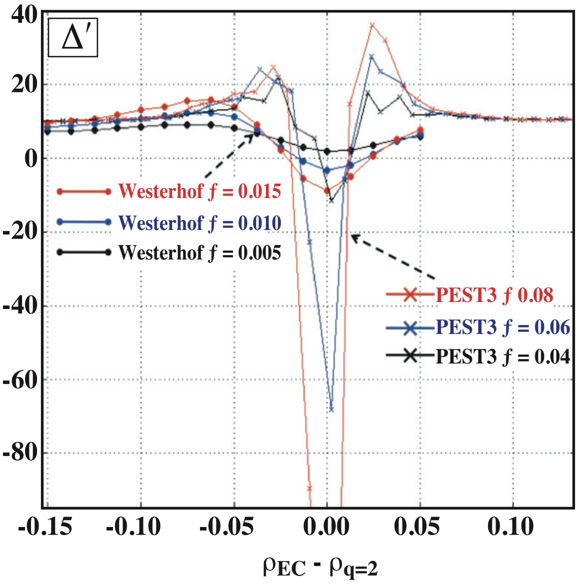

Fig. 5. Δ´ values from the analytical calculation for cylindrical geometry in Ref. 6 (circles) and from the PEST3 calculations (crosses) for three amplitudes of current perturbations.

References

1. L.L. Lao *et al.*, Nucl. Fusion **30**, 1035 (1990).
2. A. H. Glasser and M. S. Chance, Bull. Am. Phys. Soc. **42**, 1848 (1997).
3. L.C. Bernard, *et al.*, Comput. Phys. Commun. **24**, 377 (1981).
4. A. Pletzer, *et al.*, J. Comput. Phys. **115**, 530 (1994).
5. D.P. Brennan, *et al.*, Phys. Plasmas **9**, 2998 (2002).
6. E. Westerhof, Nucl. Fusion **30**, 6 (1990).